Article:
Yang, D, Ghadiri, M orcid.org/0000-0003-0479-2845, Sun, Y et al. (3 more authors) (2018) Critical electric field strength for partial coalescence of droplets on oil–water interface under DC electric field. Chemical Engineering Research and Design, 136. pp. 83-93. ISSN 0263-8762

https://doi.org/10.1016/j.cherd.2018.05.004

Critical Electric Field Strength for Partial Coalescence of Droplets on Oil-Water Interface under DC Electric Field

Donghai YANG[a, c], Mojtaba GHADIRI[b, *], Yongxiang SUN[a, c], Limin HE[a, c], Xiaoming LUO[a, c], Yuling LÜ[a, c]

([a] College of Pipeline and Civil Engineering, China University of Petroleum, Qingdao 266580, Shandong, PR China

[b] Institute of Particle Science and Engineering, University of Leeds, Leeds LS2 9JT, UK

[c] Shandong Provincial Key Laboratory of Oil & Gas Storage and Transportation Safety, China University of Petroleum, Qingdao 266580, P R China)

Corresponding Author is Mojtaba Ghadiri Tel：+44 113 343 2406 Fax：+44 113 343 2384 E-mail：M.Ghadiri@leeds.ac.uk

Abstract

Water droplets dispersed in crude oil have to be separated before processing and this is most commonly done by electrical dehydration. Under high strength electric fields, partial coalescence may occur. The critical electric field strength for partial coalescence occurance depends on several factors. In this paper, the effects of droplet diameter, conductivity, permittivity and other physical properties, such as viscosity, density and interfacial tension, on critical electric field strength have been studied experimentally, based on which a formula to predict the electric field strength is proposed. The critical electric field strength is shown to vary with the inverse of the square root of droplet radius, $R^{-0.5}$. Its value is lower for droplets with high surfactant concentration. As the surfactant concentration increases, the slope $E_{crit}/ R^{-0.5}$ (k) decreases. The critical electric field strength increases as the concentration of alkali is increased. The slope k increases with the increase of conductivity and alkali concentration. On adding polymer, the critical electric field intensity is much higher than that of distilled water, and this suggests that droplets containing polymer do not

easily form secondary droplets. The slope k increases with the increase of polymer concentration. The density difference and oil viscosity also affect E_{crit}, which is proportional to the product of density difference and oil viscosity. Based on experimental data a formula expressing the critical electric field strength is obtained by linear fitting . The slope is the same for the same oil but intercept is different for water containing different additives.

Key words: Critical electric field strength; Droplet; Coalescence; Interface; Direct current

Nomenclature

a	Intercept
A	The projected area of the droplet, m^2
b	Slope
Bo	Bond number
C_d	Drag coefficient
E	Electric field strength, $v \cdot m^{-1}$
E_{crit}	Critical electric field strength, $v \cdot m^{-1}$
F_A	Virtual mass force, N
F_B	Buoyancy force, N
F_D	Drag force, N
F_E	Electric force, N
g	Gravitational acceleration, $m \cdot s^{-2}$
H	Thickness, m
G	Gravity force, N
k	Slope of E_{crit} and $R^{-0.5}$, $v \cdot m^{-0.5}$
Oh	Ohnesorge number

ΔP	Additional pressure, N
Q	charge, C
R	radius, m
Re	Reynolds number
U	Applied voltage, V
We	Weber number
WO	Weber number multiplied by Ohnesorge number

Greek symbols

ρ	Density, $kg \cdot m^{-3}$
$\Delta\rho$	Density difference, $kg \cdot m^{-3}$
ρ_*	Density ratio
μ	Viscosity, Pa·s
μ_*	Viscosity ratio, Pa·s
σ	Interfacial tension, $N \cdot m^{-1}$
φ	Induced charge, C
θ	Angle between the electric field direction and the droplet radius, °
ε	Relative permittivity
ε_0	Permittivity of free space， $F \cdot m^{-1}$
κ	Conductivity, $S \cdot m^{-1}$

Super/subscripts

1	Water phase
2	Continuous phase

1. Introduction

Water droplets dispersed in dielectric fluids, like water-in-oil emulsions, ccommonly exist in the oil and chemical industries[1-3]. When the droplets come in contact with the bulk oil and water interface, the film between the droplet and interface starts thinning and eventually ruptures. The droplet coalesces with the bulk water. There

are two mechanisms for coalescence: complete coalescence, in which the droplet merges with the continuous phase; and partial coalescence, where a smaller secondary droplet[4-8] is produced. Charles and Mason[4,5] were the first to report on droplet-interface partial coalescence. They attributed the process to Rayleigh–Plateau instability generated by capillary waves. As the liquid film between the droplet and interface ruptures, rapid expansion of the contact region gives rise to a surface capillary wave that propagates up the droplet surface, eventually converging to elongate the droplet at its top. Simultaneously, capillary pressure inside the droplet and gravity drains the droplet fluid into the bulk. These two competing process result in a decreasing droplet neck, and eventual fluid break-up due to the instability. However, Blanchette and Bigioni[6] proposed a different mechanism of partial coalescence which is opposed to the Rayleigh–Plateau instability mechanism. Instead they suggested the partial coalescence to be dependent on the rates of vertical and horizontal collapse, when gravitational effects are negligible. Under these conditions, to get secondary droplet, the vertical collapse rate has to be sufficiently slow. Paulsen[7] and Chen[8] also supported this mechanism.

Chen[8]found the process of partial coalescence can be devided into two stages: propagation of surface waves and capillary pinch-off. The first stage is the same as the description of Charles and Mason[4,5], which is related with Rayleigh–Plateau instability. In the second stage, the column, caused by the uplifting effect of the capillary wave at droplet top, becomes sufficiently thin for capillary instability to set in. A neck forms

near the base of the column, and eventually a secondary droplet pinches off.

There are four dimensionless numbers of the system governing coalescence patterns: the Ohnesorge number Oh, the Bond number Bo, and the density and viscosity ratios[6,7,9] between the droplet and the continuous phases:

$$\mathrm{Bo}=\frac{\Delta\rho g R^2}{\sigma} \tag{1}$$

$$\mathrm{Oh}=\frac{\mu_1}{\sqrt{(\frac{\rho_1+\rho_1}{2})\sigma}} \tag{2}$$

$$\rho_*=\frac{\rho_1}{\rho_2} \tag{3}$$

$$\mu_*=\frac{\mu_1}{\mu_2} \tag{4}$$

where subscripts 1 and 2 represent the droplet and continuous phases, ρ is density and $\Delta\rho=\rho_1-\rho_2$, g is gravitational acceleration, σ is interfacial tension, and μ is viscosity.

The critical Oh number for partial coalescence is about 0.03[6,10]. Mohamed-Kassim and Longmire[11] found that partial coalescence occurs if $\mathrm{Bo}\cdot\mathrm{Oh}<0.02–0.03$. However, Chen[8] observed complete coalescence for a much lower $\mathrm{Bo}\cdot\mathrm{Oh}=3.19\times10^{-6}$, so the critical value is different for different materials.

Chen[9] reported partial coalescence occurs for an intermediate range of droplet sizes; it is demoted by water viscosity for smaller droplets and by water density for larger ones. Blanchette and Bigioni[6] found the viscosity of the liquid determines the extent of capillary waves propagating. For very viscous liquids, capillary waves are damped, leading to complete coalescence. The critical Ohnesorge number shows a weak dependence on gravitational effects, and was found to be 0.026±0.001 when gravity was negligible.

Paulsen et al.[7] studied the effect of viscosity, interfacial tension, droplet diameter and distance between droplet and interface. They found capillary waves are visible in the less viscous continuous phase. Blanchette et al.[12] found that the interfacial tension ratio between droplet and continuous phase also affected the interface coalescence.

Electro-dehydration is a common method which is used to separate water from oil[3]. Under electric field, the electrostatic pressure applied on the interfaces can significantly change the droplet shape and, even, result in interface instability [13]. This instability will generate a liquid bridge between droplet and interface, which can enhance droplet-interface coalescence[14]. But unfortunately, when electric field strength is high enough, only a part of droplet can merge into the bulk phase, which is partial coalescence [15-18]. Also non-coalescence or bounce can occur when droplet falling on the flat interface[18-22].

The coalescence pattern depends on electric field strength and physical properities, such as conductivity, permittivity, viscosity etc. Hamlin et al. [18] found the coalescence pattern went through complete coalescence, partial coalescence and non-coalescence with increasing electric field strength under DC electric fields. The conductivity plays an important role in the process of partial coalescence. There is a threshold value above which the droplet bounce off. Some literature [20, 21, 23, 24] reported that the coalescence pattern can be tuned from coalescence to non-coalescence. The coalescence pattern is also related with the properties of the oil phase. Experiments have been conducted with sunflower oil, mineral oil or white oil[26,27]. However, the droplet-interface coalescence

is complicated in crude oil, because of the presence of surface-active agents (e.g. resins and asphaltenes). This can change the properties of films and then even change the stability of droplet and coalescence characteristics. Svein et al.[25] conducted experiments with a near-infrared high-speed optical camera to record the coalescence of a droplet falling onto a bottom droplet in crude oil. The droplet was stable on the interface because of the rigid film formed by surface-active compounds without electric field. When the electric field was applied, the falling droplet merged with the bottom droplet. Partial coalescence was observed at 60℃, and non-coalescence occurred at 40℃, which resulted from the charge transfer through a thin liquid bridge formed by resins and asphaltenes connecting the two droplets

Partial coalescence produces very small droplets, which is undesirable as they are more difficult to remove from oil. Mousavichoubeh[17] used the product of Weber number ($We=2R\varepsilon_2\varepsilon_0E^2/\sigma$) and Ohnesorge number (Oh) to get a new dimensionless number WO, with which the volume of the secondary droplets was correlated. WO number represents the dominance between the necking process caused by electric stress and pumping process driven by the interfacial tension and retarted by the viscous effect. There is a tendency that increasing the electric field strength results in increasing the radius of secondary droplet[16-18]. Mousavichoubeh et at.[17] found that with increasing concentration of the surfactants, the volume of secondary droplets increased. The volume of secondary droplets has been reported to be dependent on the initial droplet size, electric field strength and the distance between the droplet and the interface[16,17],

conductivity of water[18], permittivity[15] , viscosity[15], interfacial tension [15, 17] etc.

Aryafar and Kavehpour[15] investigated the influence of electric field strength, viscosity and interfacial tension on droplet-interface coalescence. The viscosity had no effect on partial coalescence. Decreasing the permittivity of water droplets resulted in a decrease of the critical electric field. The critical field strength for partial coalescence was found to dependend on interfacial tension, droplet diameter and permittivity. If the field was increased further above the threshold for partial coalescence, fluid jet occurred and very fine droplets were produced. Electric field strength should be set at a lower value than the threshold one for partial coalescence when designing electrocoalescence dehydrator. This is because secondary droplets can be very difficult to separate. The increase of electric field strength, droplet diameter [16-18], water permittivity[15] and decrease of interfacial tension[15, 17], and conductivity[18] all enhance the formation of secondary droplets.

The critical electric field is important for electro-dehydrator design, above which the droplet may experience partial coalescence[15]. Some experimental and simulation results suggested that the critical electric field strength is $E_{\text{crit}}=\sqrt{\frac{C\sigma_{12}}{\varepsilon_2 R}}$ where σ_{12} is interfacial tension, C is a constant and ε is permittivity. The exact value of C is about 0.204[28,29]. If there is a fluid/fluid interface between two insoluble fluids, the gravity plays important role and $E_{\text{crit}}=(\frac{2}{\varepsilon_2})^{0.5}[(\rho_1-\rho_2)g\sigma_{12}]^{0.25}$ [30] . When the applied electric field is parallel to a fluid jet in an immiscible medium, the critical electric field strength is $E_{\text{crit}}\approx(\frac{2\pi\sigma_{12}}{(\varepsilon_1-\varepsilon_2)R})^{0.5}$[31].

It is apparent that the critical electric field strength for partial coalescence is dependent on the interfacial tension, permittivity, droplet radius and density. However, the effects of viscosity and conductivity are lacking in this consideration. Moreover the physical properties of the water phase particularly regarding the alkali-surfactant-polymer (ASP) flooding in the area of enhanced oil recovery (EOR) are complex. Also, most results are qualitative and cannot give quantitative prediction of critical electric field strength. It is therefore desirable to analyse the effect of interfacial tension, permittivity, conductivity, density and viscosity on the critical electric field strength for partial coalescence. In this paper, the physical properties of the water phase are tuned by adding alkali, surfactant and polymer to investigate the effect of interfacial tension, conductivity, density and viscosity on the critical electric field strength under DC electric filed. Five types of silicon oil have been used for this purpose.

2.Theory

When a droplet rests on the oil-water interface in an electric fields, there are several forces acting on droplet, such as electric force $F_{E,}$ additional pressure ΔP due to interfacial tension, gravity force G, buoyancy force $F_{B.}$ At the moment of coalescence there is drag force F_D applied on droplet. Ther forces are shown in Fig. 1.

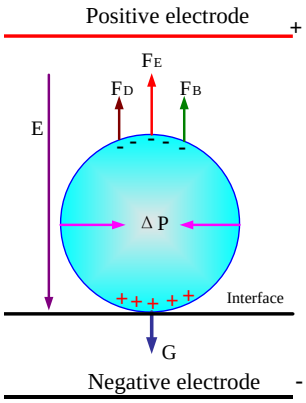

Fig. 1. Forces on droplet in electric field

The droplet is polarized when the electric field is applied and charges are redistributed; therefore the shape of the droplet becomes ellipsoidal by the action of the electric field force. Acoording to Xu and Chen's work [32], the electric field force applied on unit area of the droplet, calculating calculated by using method of virtual work, is

$$\frac{\mathrm{d}F}{\mathrm{d}A}=\frac{9}{2}\varepsilon_0\varepsilon_2 E^2\cos^2\theta \tag{5}$$

where ε_0 and ε_2 are permittivity of vacuum and oil matrix, respectively; E is the electric field strength and θ is the angle between the electric field direction and the droplet radius pointed from the center of sphere to the unit surface area.

Hence, the projection of the whole electric field force that the conductive droplet receives on the direction of the applied electric field is

$$F_{\mathrm{E}}=\int_A \left(\frac{9}{2}\varepsilon_0\varepsilon_2 E^2\cos^2\theta\right)\cos\theta\,\mathrm{d}A=\frac{9}{4}\pi\varepsilon_0\varepsilon_2 E^2R^2 \tag{6}$$

where A is the projected area of the droplet and R is the initial radius of the droplet.

The droplet with radius R could keep its spherical shape due to the capillary pressure against the additional pressure ΔP, which is given by the Young–Laplace equation:

$$\Delta P = \frac{2\sigma}{R} \tag{7}$$

As is shown in Fig. 1, at the moment of coalescence there is relative movement between droplet and the continuous fluid, the drag force F_D of the fluid on the droplet in the opposite direction of its movement occurs. In this work, the effect of internal circulation in the droplet is neglected, and the drag force F_D [33] is given as:

$$F_D = \frac{1}{2}\rho_2 C_d A v^2 = \frac{6\pi\mu_2 R\rho_2}{\rho_1} v \tag{8}$$

where $C_d = \frac{24}{Re}$ is the drag coefficient.

The buoyancy force F_B acts in the opposite direction of gravity, which can be expressed as:

$$F_B = \rho_2 g V_d \tag{9}$$

where V_d is the droplet volume.

As is shown in Fig.1, gravity force G expressed as follows:

$$G = \rho_1 g V_d \tag{10}$$

When electric field strength is low, the electric force is less than the sum of other forces. As electric field strength increases, the electric force exceeds other forces, and the first secondary droplets form at the upper point. This strength is the critical electric field strength E_{crit}. From Eq.5 to Eq.10, the critical electric field strength is dependent on

$$E_{crit} = f(R, (\rho_1 - \rho_2), \sigma, \mu_2, \varepsilon_2) \tag{11}$$

When the electric filed strength is higher than a critical value, the electrostatic pressure will stretch the upper part of falling droplet and then give rise to the formation

of columnar shape. This column experiences a pinch-off and a secondary droplet or fine droplets are produced, as is shown in Fig. 2. In this paper this functional form is experimentally quantified.

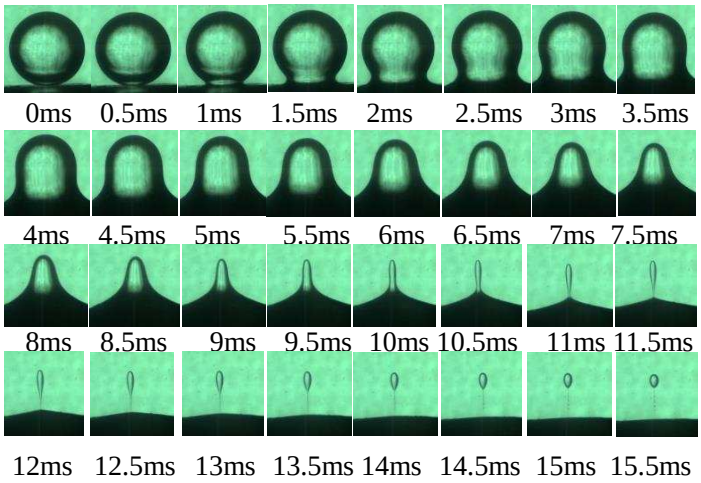

Fig. 2. Partial coalescence of distilled water on the interface of water-silicon oil 1 (E=240.5kV·m^{-1}, d=1280μm)

3.Experimental set-up and procedures

The experimental set-up is the same as that used in previous work[16.17.22]. The cell is made of Perspex for the observation of experiment. The high voltage and ground electrodes are both polished brass plates with dimensions of 90 mm × 25 mm. The high voltage electrode is attatched to the upper part of the cell, which can be moved to change the distance and the electric field strength. There is a small hole through the mid-point of the upper part and brass plate to allow a hypodermic needle to pass through it. The needle, attached to a syringe (Hamilton micro-liter syringe) is used to introduce small aqueous droplets in the cell on the interface. The needle is grounded to ensure that the droplets are uncharged. The high voltage electrode is connected to a positive polarity

high voltage direct current power amplifier (TREK 20/20C) and the bottom electrode is grounded. A high-speed digital video camera (Photron FASTCAM SA5), equipped with a micro lens (NAVITAR 12× Zoom Lens) was used to observe the coalescence phenomenon within the cell and it was focused on the centre of the water-oil interface.

In this work the bottom half of the cell is filled with water and the top half with oil to form an interface of two phases. In the experiments, silicon oils were used. A halogen cold lamp (Dedolight DLHM4-300) with four flexible fibre optic heads was used for lighting. The surfactant (Tween 80), alkali (Na_2CO_3) and polymer (HPAM, partially hydrolysed polyacrylamide), all obtained from Sigma Inc,were added to the distilled water to tune the surface tension, conductivity and viscosity of dispersed phase. Different oils, as described in Table 1 were used to get different density, viscosity and surface tension of continuous phase. The mass fractions of Tween 80 solution were 10, 20, 30 and 100 ppm. The mass fractions of Na_2CO_3 solution were 100, 250, 500, 1000 and 2000 ppm.The mass fractions of HPAM were 50, 100, 200, 400 and 600 ppm.

The viscosity of liquids were measured using Bohlin CVO rheometer (Malvern Instruments Inc). The density was measured by using a volumetric flask. The conductivities of liquids were measured by using a conductivity indicator (Model 4310, Jenway Products Inc). The permittivities of oil were obtained from the literature[35] and the supplier. The interfacial tensions were measured using a contact-angle measuring instrument EasyDrop (Kruss GmbH Inc).

The properties of the liquids used in this research and interfacial tension values for

solutions are given in Tables 1 to 5, respectively, where further details of the experimental procedure are given.

Table1 Properties of oil and water

Liquids	Conductivity ($\mu S \cdot cm^{-1}$)	Viscosity (mPa·s)	Density ($kg \cdot m^{-3}$)	Surface tension $mN \cdot m^{-1}$	Permittivity
Distilled water	1.00	1.270	1000.00	72.00	80.00
silicon oil 1	2.32×10^{-7}	56.990	950.00	19.91	2.700
silicon oil 2	2.33×10^{-7}	102.960	954.00	20.13	2.707
silicon oil 3	2.31×10^{-7}	171.660	960.00	20.24	2.714
silicon oil 4	2.35×10^{-7}	239.220	965.00	20.44	2.717
silicon oil 5	2.33×10^{-7}	304.700	970.00	21.00	2.720

Table 2 The physical properties of water solution with surfactant

Liquids	Conductivity ($\mu S \cdot cm^{-1}$)	Viscosity (mPa·s)	Density ($kg \cdot m^{-3}$)	Surface tension $mN \cdot m^{-1}$	Permittivity
Tween80 10 ppm	1.23	1.269	998.056	63.4	≈80
Tween80 20 ppm	1.47	1.258	998.113	58.5	≈80
Tween80 30 ppm	1.56	1.267	998.169	56.3	≈80
Tween80 100 ppm	1.71	1.271	998.565	55.9	≈80

Table 3 The physical properties of water solution with Na_2CO_3

Liquids	Conductivity ($\mu S \cdot cm^{-1}$)	Viscosity (mPa·s)	Density ($kg \cdot m^{-3}$)	Surface tension $mN \cdot m^{-1}$	Permittivity
Na_2CO_3 100 ppm	243.00	1.254	998.18	71.50	≈80
Na_2CO_3 250 ppm	400.00	1.243	998.45	71.70	≈80
Na_2CO_3 500 ppm	1234.00	1.267	998.90	71.40	≈80
Na_2CO_3 1000 ppm	2250.00	1.279	999.80	71.60	≈80
Na_2CO_3 2000 ppm	4100.00	1.243	1005.53	71.80	≈80

Table 4 The physical properties of water solution with HPAM

Liquids	Conductivity ($\mu S \cdot cm^{-1}$)	Viscosity (mPa·s)	Density ($kg \cdot m^{-3}$)	Surface tension $mN \cdot m^{-1}$	Permittivity
HPAM 50 ppm	18.88	5.930	998.24	71.20	≈80
HPAM 100 ppm	31.40	9.480	998.52	70.60	≈80
HPAM 200 ppm	67.40	17.450	998.68	70.80	≈80
HPAM 400 ppm	109.20	28.310	999.94	70.15	≈80
HPAM 600 ppm	145.40	36.810	1000.92	67.60	≈80

Table 5 Interfacial tension of oils and water

Materials	σ/$mN \cdot m^{-1}$	Materials	σ/$mN \cdot m^{-1}$

silicon oil 1+distilled water	39.81	silicon oil 1+Tween 80 10 ppm	33.81
silicon oil 2+distilled water	40.01	silicon oil 1+Tween 80 20 ppm	28.72
silicon oil 3+distilled water	40.21	silicon oil 1+Tween 80 30 ppm	25.02
silicon oil 4+distilled water	40.38	silicon oil 1+Tween 80 100 ppm	20.20
silicon oil 5+distilled water	40.57	silicon oil 1+HPAM 50 ppm	31.01
silicon oil 1+Na_2CO_3 100 ppm	39.71	silicon oil 1+HPAM 100 ppm	30.56
silicon oil 1+Na_2CO_3 250 ppm	39.69	silicon oil 1+HPAM 200 ppm	29.71
silicon oil 1+Na_2CO_3 500 ppm	39.62	silicon oil 1+HPAM 400 ppm	28.33
silicon oil 1+Na_2CO_3 1000 ppm	39.54	silicon oil 1+HPAM 600 ppm	27.34
silicon oil 1+Na_2CO_3 2000 ppm	39.43		

Water droplets of different sizes were produced using hypodermic needles in the range 576 - 1196 μm. The diameter of the droplets was measured by Image J and PFV (Photron Fastcam Viewer ver. 320) software. The standard deviations were in the range from 1 to 4 μm from the mean diameter aspect. The diameter of the needle was measured by a microscope and was used for the in-situ calibration of the droplet size and measurements on the droplet plane. DC waveform was used to study the effect of physical properties on the formation of secondary droplets. The experiments were performed at 20±1℃.

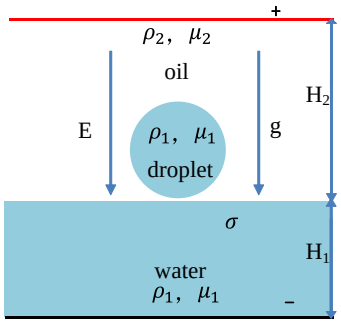

Fig. 3. The diagram of droplet on the interface

If the water droplet is a perfect conducter, like copper, the electric field applied on oil is $E=U/H_2$, as shown in Fig. 3. When droplet rest on the interface and the electric field is applid, the electric field is redistributed, resulting from the discontinuous of

permittivity. The permittivity of water is about 80, while the permittivity of oil is 2.70. Therefore, the electric field intensity can be calculated as[34]

$$E=\frac{U}{(H_2/\varepsilon_2+H_1/\varepsilon_1)\varepsilon_2} \quad (12)$$

where U: the applied voltage, V; H_2: the thickness of oil (m)- in our case: 36±0.5 mm; H_1: the thickness of water (m)- in our case: 30±0.5 mm; ε_1: the relative permittivity of water - according to Table 1: ε_1=80; ε_2: the relative permittivity of oil- in our work silicon oils were used.

4. Results and discussion

In our experiments, when the electric field strength, droplet radius or properties of droplet and oil are changed, the coalescence pattern changes as well. As shown in Fig. 4, there are two kinds of droplet-interface coalescence, complete coalescence and partial coalescence, which is dependent on electric field strength, droplet size and properties of water and oil. When the electric field strength is higher than a critical value, the droplet experiences partial coalescence, as shown in .

In order to investigate the effect of different parameters on the critical electric field strength, the experiments were conducted by tuning droplet radius, conductivity, viscosity, density difference and other physical properties. As shown in Fig. 1, when DC electric field is applied, the negative charge accumulates in the upper part of the droplet due to the polarization. When the electric field strength is low, the oil film between droplet and oil-water interface is broken and the droplet merges into the bulk water with no secondary droplet formation (Fig. 4 (a)). When the electric field strength is high, the top of the droplet is polarized with the opposite sign charges to that of upper

electrode. The capillary pressure in the droplet tends to drive fluid toward the bottom reservoir[18] during the coalescence process. Therefore, because of the two competing forces, electric force and capillary force, produce the necking process and the secondary droplets (Fig 4(b)). A typical process of partial coalescence and it is about 12 ms to form the first secondary droplet.

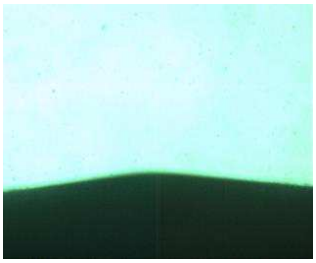

(a) Complete coalescence
E=93.15 kV·m^{-1} d=1280μm

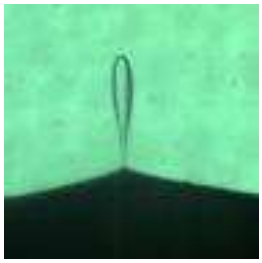

(b) Partial coalescence
E=240.5kV·m^{-1}d=1280μm

Fig. 4. Two types of droplet-interface coalescence on the interface of water-silicon oil 1

4.1 The influence of droplet radius on critical electric field strength

The silicon oil 1 and distilled water are used as the continuous and dispersed phase, respectively. When the droplet radius is changed, the additional pressure is changed. According to Eq. 7, the additional pressure increases when radius decreases. As the additional pressure is opposite to the electric field force, it is difficult to break up small droplets. As shown in Fig. 5, the critical electric field strength increases as the droplet radius decreases. The relationship between critical electric field strength (E_{crit}) and $R^{-0.5}$ is linear.

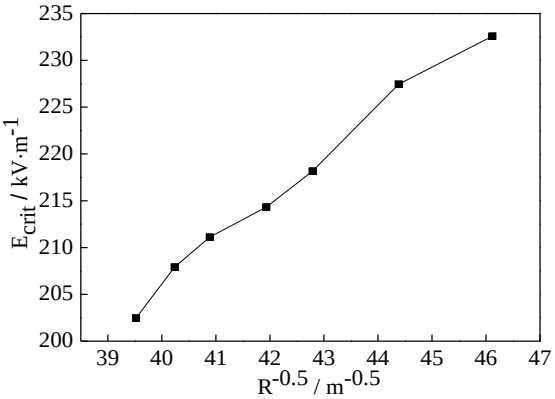

Fig. 5. Effect of radius on E_{crit} when water is distilled water

Aryafar and Kavehpour [15] introduced three relationships of the critical electric field strength in the study of droplet-interface coalescence under electric fields.

$$E_{crit} = \sqrt{\frac{C\sigma}{\varepsilon_0 \varepsilon_2 R}} \tag{13}$$

$$E_{crit} = \left(\frac{2}{\varepsilon_0 \varepsilon_2}\right)[(\rho_1 - \rho_2)g\sigma]^{1/4} \tag{14}$$

$$E_{crit} = \sqrt{\frac{2\pi\sigma}{\varepsilon_0(\varepsilon_1 - \varepsilon_2)R}} \tag{15}$$

The relationship of E_{crit} and $R^{-0.5}$ is the same in Eq. 13 and 15. However, the value of $E_{crit}/R^{-0.5}$ is different. In order to get the relationship of E_{crit} and $R^{-0.5}$, the slope of E_{crit} and $R^{-0.5}$ should be analysed. Here the slope of E_{crit} by $R^{-0.5}$ is defined as k.

4.2 Effect of interfacial tension

As shown in Eq. 13, k is related with the permittivity, droplet size and interfacial tension. With increasing surfactant concentration, the relationship of E_{crit} and $R^{-0.5}$ is the same (Fig. 6), linear, as that of distilled water.

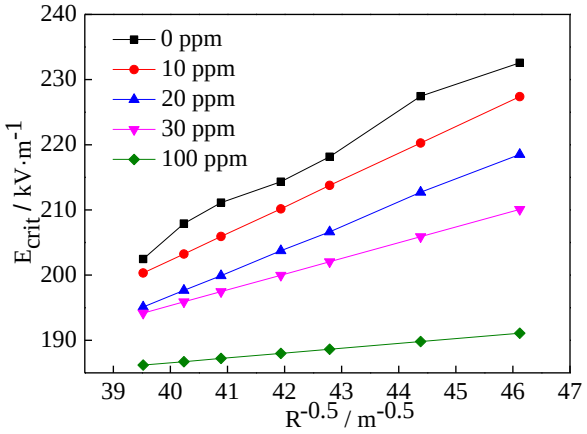

Fig. 6 Effect of diameter on E_{crit} at different surfactant concentration

With the increase of surfactant concentration and the resulting decrease of the interfacial tension of oil and water, the critical electric field strength is lowered. This is consistent with Mousavichoubeh's work[17]. With increasing concentration, the slope k decreases, which is consistent with Aryafar and Kavehpour's work [15]. The reason is that as the interfacial tension is decreased the additional pressure decreases, keeping the droplet spherical. If it is reduced, the electric force can easily stretch the droplet to be ellipsoidal, and in the case of high values, the stretched droplet disintegrates and produces fine secondary droplets. According to Aryafar and Kavehpour [15] the capillary pressure during coalescence, approximately 2σ/R, pulles the droplet to merge into the bulk liquid. When interfacial tension is low, the capillary pressure is low, which produces larger secondary dorplets. The interfacial tension of water-oil reduces after adding surfactant, and the slope k decreases. According to Eq. 13, the critical field strength is proportional to $\sigma^{0.5}$. However, experimental results show that the slope is not linear with $\sigma^{0.5}$ (Fig. 7). As surfactant is added, the density and conductivity of water both change, which may be the reason.

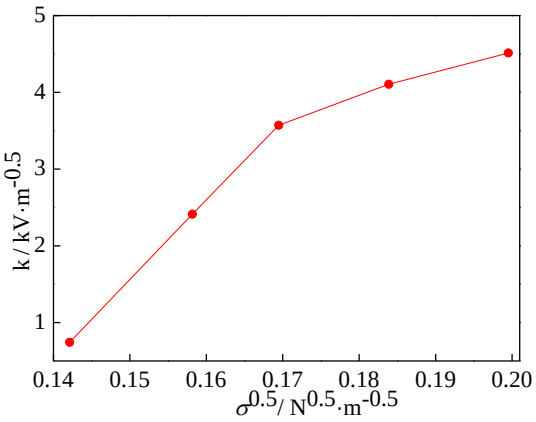

Fig. 7 Relationship between k and $\sigma^{0.5}$

4.3 The effect of conductivity

In order to explore the effect of conductivity on droplet-interface electrocoalescence, the alkali (Na_2CO_3) solution and silicon oil 1 were used. As shown in Table 3, the conductivity increases as concentration of Na_2CO_3 is increased. From Fig. 8, the critical electric field strength increases as the droplet radius is decreased and the concentration of alkali is increased. The relationship is linear between E_{crit} and $R^{-0.5}$. The slope k increasing with concentration increasing, which indicates that the higher the conductivity, the more difficult the secondary droplets formation. Hamlin [18] also reported that there existed a critical conductivity below which oppositely charged droplets only partially coalesced, which means that secondary droplets are easier to form when conductivity is low. Howerever the interfacial tension changes little afer adding alkali. With the increase of conductivity, the density and moving of charges in the droplet become faster. Consequently, the charges on the droplet bottom surface close to the interface will leak quickly into the bulk water and a stronger electrostatic

repulsion resulting from the unbalanced charge on the opposite surface of the droplet occurs, which suppress the secondary droplet formation.

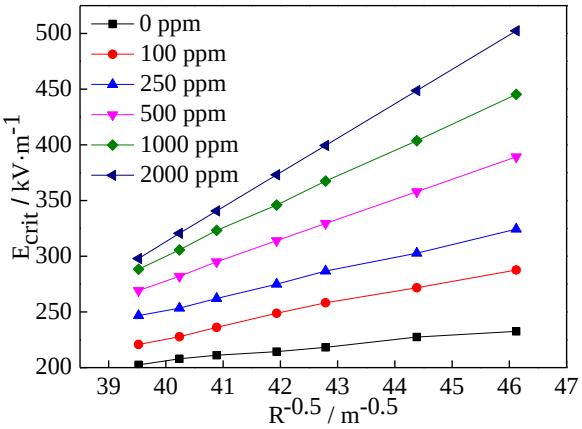

Fig. 8. Effect of radius on E_{crit} at different Na_2CO_3 concentration

As shown in Fig. 1, the negative charge accumulates in the upper part of the droplet for the polarization when DC electric field is applied, with the upper electrode being positive. The negative charge remaining near the top provides the electric force to produce the secondary droplet. When coalescing, the capillary pressure in the droplet tend to drive fluid toward the bottom reservoir[18]. Therefore, the two competing forces, electric force and capillary force, result in the formation of the secondary droplet. The electric force $F_E \propto QE$, and the capillary force is approximately $2\sigma/R$. Under the same electric field strength, in order to get the same electric force, the charge has to be the same. But when conductivity is high, the charge density of the same droplet is high, so less volume is needed to produce the same charge. Therefore, the secondary droplet can be smaller at high conductivity, which means that it is difficult to form secondary dorplet for high conductivity water. The slope k increases with the increase of

conductivity (as alkali concentration is increased) but the trend gradually slows down, as shown in Fig. 9.

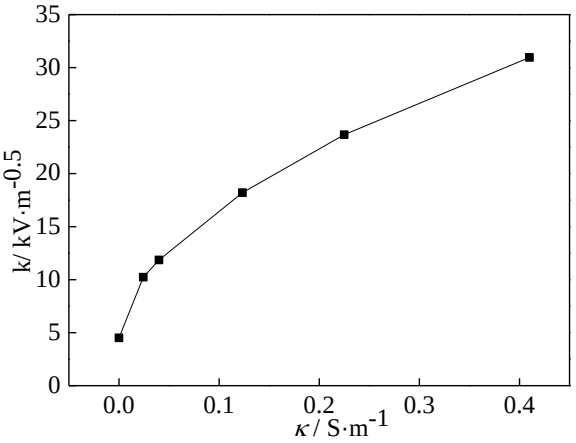

Fig. 9. Relationship between k and solution conductivity

4.4 Effect of polymer

In order to study the effect of polymer, silicone oil 1 and HPAM solution were used. The relationship of E_{crit} and $R^{-0.5}$ for several polymer concentrations is shown in Fig. 10. The trend is linear, as that of distilled water, surfactant and alkali. With adding polymer, the critical electric field intensity is much higher than that with distilled water, and this suggests that the droplet containing polymer does not easily form secondary droplets.

The polymer solution is non-Newtonian-fluid. The polymer molecules start forming long chains when the concentration of polymer is higher than the critical micelle concentration, and the polymer droplet becomes more elastic. With the increasing concentration of polymer, the elasticity of polymer droplet is more pronounced [36], and the liquid bridge breakup process is strongly resisted by the elastic

stress.

On one hand, a long chain structure is formed between the polymer molecules. The electric field has to be high enough to break up long chains between polymer molecules, which indicates that it is not easy to form a secondary droplet. On the other hand, the viscoelasticity of polymer solution increases the viscosity and breaking stress of water bridge.

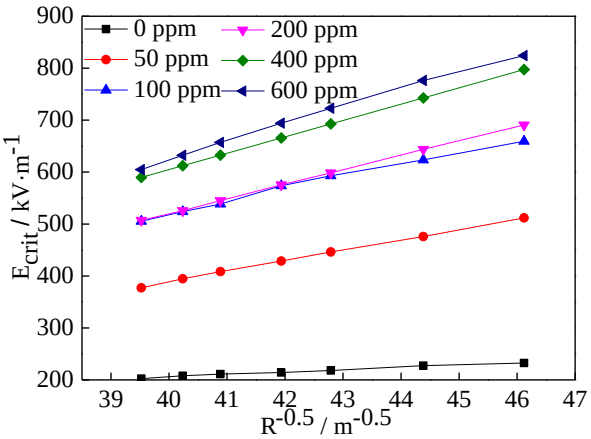

Fig. 10 Effect of radius on E_{crit} at different HPAM concentration

The relationship between k and water viscosity is shown in Fig. 11. k increases fast with the increase of viscosity, but the trend slows down gradually.

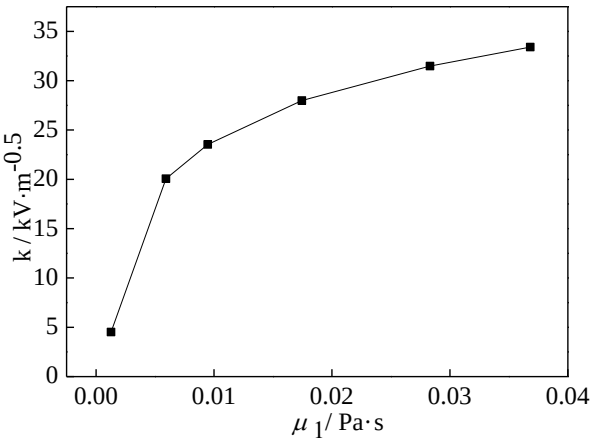

Fig. 11 Relationship between k and water viscosity

4.5 The effect of oil viscosity and density

According to the Eq. 11 and Eq. 14, the critical electric field intensity is related to the density difference of the oil and water phase and the viscosity of continuous phase. Five kinds of silicone oils were used to study the influence of these properties on the droplet-interface coalescence of distilled water droplet in silicone oils. The relationship between E_{crit} and $R^{-0.5}$ for different viscosities is shown in Fig. 12, where the increase of E_{crit} with viscosity is clearly discernable.

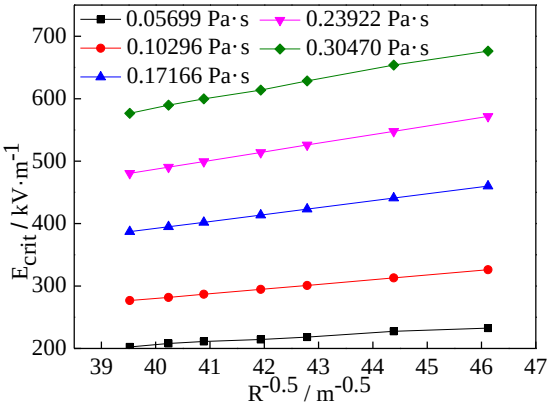

Fig. 12 Effect of oil viscosity and radius on E_{crit}

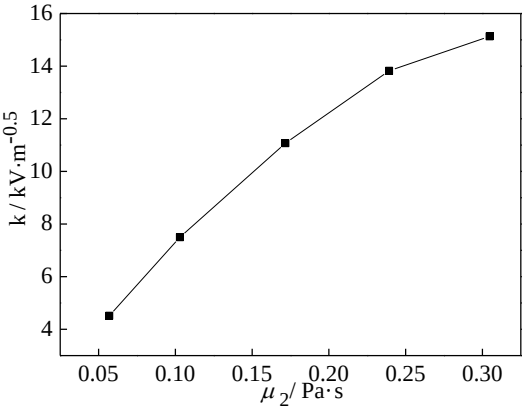

Fig. 13 Relationship between k and oil viscosity

E_{crit} is roughly proportional to $R^{-0.5}$ and the slope k increases with the increase of oil viscosity (Fig. 13). In Eq. 8, as the viscosity increases, the drag force on the secondary droplet is increased, which is different to the direction of electric force and will prevent the moving of droplet, as a result the secondary droplet formation is suppressed.

4.6 Estimation of critical electric field strength

Considering Eq. 13 and the dependence of k on the oil viscosity and density, the functional relationship between $k/(\sigma^{0.5}(\varepsilon_0\varepsilon_2)^{-0.5})$ and the product of oil viscosity and

density difference between the two phases ($\Delta\rho\mu_2$) is explored in Fig. 14 based on experimental data. Clearly a linear relationship between ($\sigma^{0.5}(\varepsilon_0\varepsilon_2)^{-0.5}$) and $\Delta\rho\mu_2$ prevails.

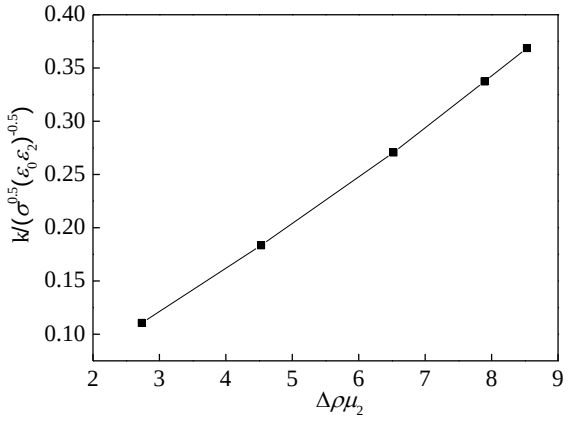

Fig. 14 Relationship between $k/(\sigma^{0.5}(\varepsilon_0\varepsilon_2)^{-0.5})$ and $\Delta\rho\mu_2$

Thus, using such a relationship

$$k \propto \Delta\rho\mu_2\sqrt{\sigma} / \sqrt{\varepsilon_0\varepsilon_2} \tag{16}$$

and taking account of dispersed phase conductivity, a functional relationship is obtained between $k/(\Delta\rho\mu_2\sigma^{0.5}(\varepsilon_0\varepsilon_2)^{-0.5})$ with a power index of 0.32, as shown in Fig. 15.

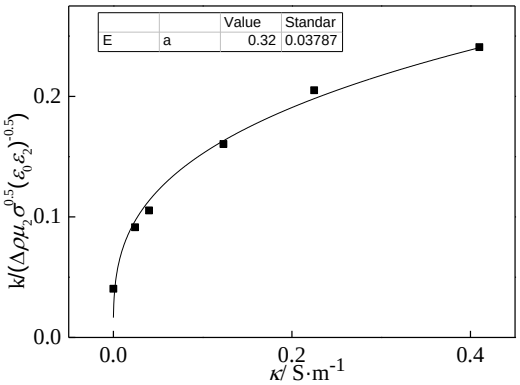

Fig. 15 Relationship between $k/(\Delta\rho\mu_2\sigma^{0.5}(\varepsilon_0\varepsilon_2)^{-0.5})$ and conductivity

According to the above results and considering that k is the slope of E_{crit} by $R^{-0.5}$, we can get

$$E_{crit} \propto \kappa^{0.32}\Delta\rho\mu_2\sqrt{\sigma}/\sqrt{\varepsilon_0\varepsilon_2 R} \tag{17}$$

The intercept and the slope can then be obtained by linear regression

$$E_{crit} = a + b\kappa^{0.32}\Delta\rho\mu_2\sqrt{\sigma}/\sqrt{\varepsilon_0\varepsilon_2 R} \tag{18}$$

This is shown in Fig. 16 for Silicon oil 1 with distilled water and various concentrations of Tween 80 solution are taken as examples.

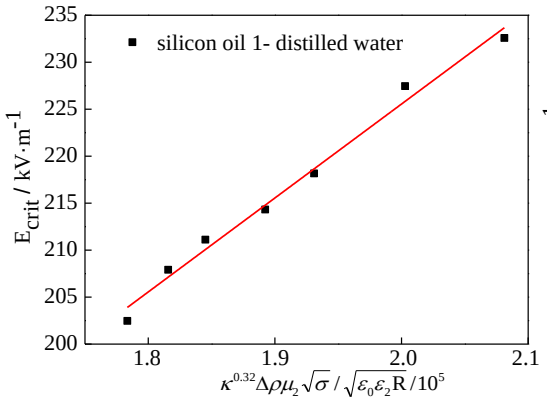

(a) Silicon oil 1 and distilled water

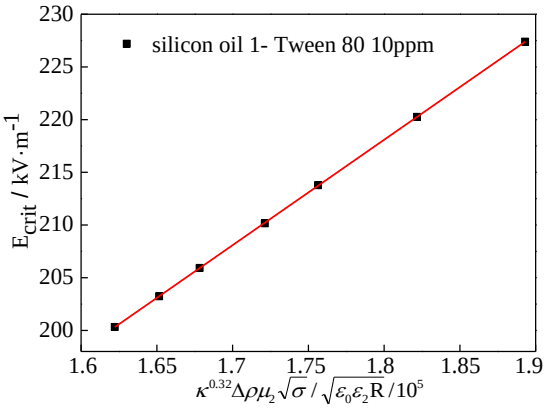

(b) Silicon oil 1 and water containing 10 ppm surfactant

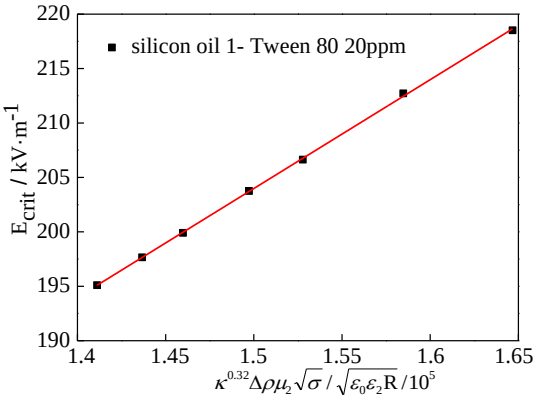

(c) Silicon oil 1 and water containing 20 ppm surfactant

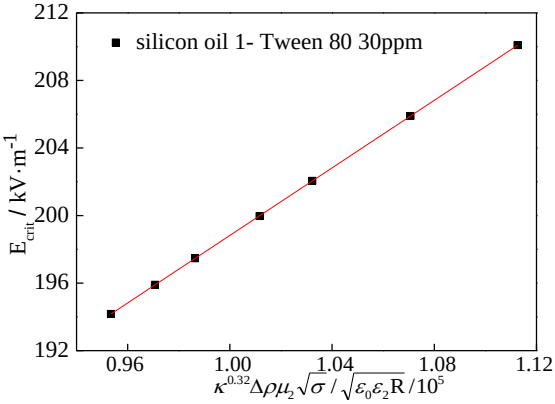

(d) Silicon oil 1 and water containing 30 ppm surfactant

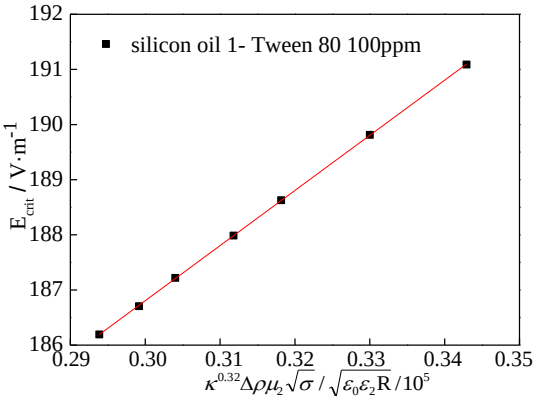

(e) Silicon oil 1 and water containing 100 ppm surfactant

Fig. 16 Linear regression of E_{crit} and $\kappa^{0.32}\Delta\rho\mu_2\sqrt{\sigma}/\sqrt{\varepsilon_0\varepsilon_2 R}$ for water with different surfactant concentrations

The slope b is about 0.001, while intercept a is different for different surfactant concentrations. When surfactant is added in the water, the surfactant molecules adsorb on the oil-water interface.The polarization and charge redistribution in the droplet will affect the breakup of liquid bridge and the intercept is affected by this.

The slope, intercept and R-square are shown in Table 6 for the systems investigated. For silicon oil 1, the slope b is 0.001, but the intercept is different. For other four silicon oils, the slope is about 0.0008 and the intercept is different. This indicates that the slope is different for different oils. As dicussed, the component of water can change the breakup characteristics of liquid bridge and affect the intercept. Ions, produced by dissociation of alkali in water droplet, and the adsorption of polymer on the surface will change the re-distribution of charges. This will change the relationship of critical electric field strength and physical properties. Though the intercept is different, E_{crit} is proportional to $\kappa^{0.32}\Delta\rho\mu_2\sqrt{\sigma}/\sqrt{\varepsilon_0\varepsilon_2 R}$ under different conditions.

Table 6 The fitted value for different materials

Materials	b	a	R-Square
Silicon oil 1+distilled water	0.0010	25.56	0.98
Silicon oil 1+Tween 80 10 ppm	0.0010	38.08	0.99
Silicon oil 1+Tween 80 20 ppm	0.0010	53.98	1.00
Silicon oil 1+Tween 80 30 ppm	0.00099	98.84	1.00
Silicon oil 1+Tween 80 100 ppm	0.00099	156.81	0.99
Silicon oil 1+Na_2CO_3 100 ppm	0.0010	-182.35	0.99
Silicon oil 1+Na_2CO_3 250 ppm	0.0010	-222.41	0.99
Silicon oil 1+Na_2CO_3 500 ppm	0.00099	-449.69	0.99
Silicon oil 1+Na_2CO_3 1000 ppm	0.0010	-646.32	0.99
Silicon oil 1+polymer 50 ppm	0.0010	-413.32	0.99
Silicon oil 1+polymer 100 ppm	0.0010	-420.64	0.98
Silicon oil 1+polymer 200 ppm	0.0010	-599.14	0.99
Silicon oil 1+polymer 400 ppm	0.0010	-654.56	1.00
Silicon oil 1+polymer 600 ppm	0.0010	-710.57	0.99
Silicon oil 2 +distilled water	0.00079	-19.75	0.99
Silicon oil 3 +distilled water	0.00081	-50.59	0.99
Silicon oil 4 +distilled water	0.00083	-65.73	0.99
Silicon oil 5 +distilled water	0.00084	-19.74	0.99

Conclusions

The critical electric field strength for the occurance of partial coalescence depends on several factors, such as droplet diameter, conductivity, permmitivity, viscosity etc. In this work, the physical properties of water were tuned by adding alkali, surfactant and polymer to investigate the effect of interfacial tension, permittivity and viscosity on critical electric field strength under DC electric field. Different types of oil have also been used to investigate the effect of oil density and viscosity.

The relationship between the critical electric field strength and droplet radius, permittivity, conductivity, viscosity, interfacial tension and density difference has been established experimentally. The relationship between E_{crit} and $R^{-0.5}$ is linear, with slope k, as also previously reported in the literature. When surfactant Tween 80 is added to

water, the critical electric field strength is lowered. As the surfactant concentration increases, the slope k decreases. When alkali is added to water, the conductivity increases. resulting in the critical electric field strength increasing. This implies that the secondary droplets do not readily form when conductivity is high. The slope k increases with the increase of conductivity and alkali concentration. It also increases with the increase of polymer content. With adding polymer, the critical electric field intensity is much higher than that of distilled water, and this suggests that droplets containing polymer do not easily form secondary droplets. Different silicon oils were used to study the effect of oil properties. The slope k increases with the increase of oil viscosity and density difference. E_{crit} is proportional to $\kappa^{0.32}\Delta\rho\mu_c\sqrt{\sigma}/\sqrt{\varepsilon_0\varepsilon_c R}$ under a wide range of conditions, based on which the equation to describe the critical electric field strength is obtained by linear regression. The slope is the same for the same oil but intercept is different for water having different additives, as they can change the breakup characteristics of the liquid bridge. Ions, produced by dissociation of alkali in water droplet, and the adsorption of polymer on the surface will change the re-distribution of charges, affecting the critical electric field strength.

The proposed equation takes account of the relevant parameters, albeit in an empirical way. However, the underlying mechanism and processes in the effect of additives on water bridge breakup characteristics requires further study.

Acknowledgements

This work was carried out at the University of Leeds, where the first author spent

a year supported by grants from the National Natural Science Foundation of China (Grant No. 51704318), the Shandong Provincial Natural Science Foundation, China (Grant No. ZR2017BEE008) and the Fundamental Research Funds for the Central Universities of China (Grant No. 16CX02001A, 15CX08008A). Introduction of Talent Research Start-up Fund (Grant No. YJ201601016). The authors would like to thank Drs Ali Hassanpour, Vincenzino Vivacqua, Umair Zafar and Mehrdad Pasha.

References

[1] J. Sjoblom, E.E. Johnsen, A. Westvik, M.H. Ese, J. Djuve, I.H. Auflem, et al. , In Encyclopedic Handbook of Emulsion Technology, edited by J. Sjoblom; New York: Marcel Dekker., 2 ed, 2001.

[2] J.S. Eow, M. Ghadiri, A.O. Sharif, T.J. Williams, Electrostatic enhancement of coalescence of water droplets in oil: a review of the current understanding, Chem. Eng. J. 84 (2001) 173-192.

[3] J.S. Eow, M. Ghadiri, Electrostatic enhancement of coalescence of water droplets in oil: A review of-the technology. Chem. Eng. J. 85 (2002) 357-368.

[4] G. E.Charles, S. G. Mason, The mechanism of partial coalescence of liquid drops at liquid/liquid interfaces, J. Colloid Sci. 15 (1960) 105–122.

[5] G. E. Charles, S. G. Mason, The coalescence of liquid drops with flat liquid/liquid interfaces, J. Colloid Sci. 15 (1960) 236–267.

[6] F. Blanchette, T. P. Bigioni, Partial coalescence of drops at liquid interfaces, Nat. Phys. 2(4) (2006) 254–257.

[7] J.D. Paulsen，R. Carmigniani，A. Kannan，J.C. Burton，S.R. Nagel, Coalescence of bubbles and drops in an outer fluid, Nat. Commun. 5 (2014) 3182-3182.

[8] X.P. Chen, S. Mandre, J. J. Feng, Partial coalescence between a drop and a liquid-liquid interface, Phys. Fluids 18 (2006) 051705.

[9] X.P. Chen, S. Mandre, J. J. Feng, An experimental study of the coalescence between a drop and an interface in Newtonian and polymeric liquids, Phys. Fluids 18 (2006) 4173-4180.

[10] B. Ray, G. Biswas, A. Sharma, Generation of secondary droplets in coalescence of a drop at a liquid-liquid interface, J. Fluid Mech. 655 (2010) 72-104.

[11] Z. Mahamed-Kassim, E. K. Longmire, Drop coalescence through a liquid-liquid interface, J. Fluid Mech. 16 (2004) 2170-2181.

[12] F. Blanchette, L. Messio, J. W. M. Bush, The influence of surface tension gradients on drop

coalescence, Phys. Fluids 21 (2009) 072107.

[13] P. Atten, F. Aitken, Electrocoalescence criterion for two close anchored water drops and estimate for pairs of drops in a field, IEEE Transactions on Industry Applications 46 (2010) 1578–1585.

[14] L.E. Lundgaard, G. Berg, S. Ingebrigtsen, P. Atten, Electrocoalescence for oil–water separation: fundamental aspects, In: Sjöblom J (ed) Emulsion and emulsion stability. Taylor and Francis, Boca Raton, 2006, 549–592

[15] H. Aryafar, H.P. Kavehpour, Electrocoalescence: effects of DC electric fields on coalescence of drops at planar interfaces, Langmuir 25 (2009) 12460–12465.

[16] M. Mousavichoubeh, M. Ghadiri, M. Shariaty-Niassar, Electro-coalescence of an aqueous droplet at an oil–water interface, Chem. Eng. Proc. Proc. Intens. 50 (2011) 338–344.

[17] M. Mousavichoubeh, M. Shariaty-Niassar, M. Ghadiri , The effect of interfacial tension on secondary drop formation in electro-coalescence of water droplets in oil, Chem. Eng. Sci. 66 (2011) 5330–5337.

[18] B.S. Hamlin, J.C. Creasey, W.D. Ristenpart, Electrically tunable partial coalescence of oppositely charged drops, Phy.s Rev. Lett. 109 (2012) 094501.

[19] R.S. Allan, S.G. Mason, Particles motions in sheared suspensions. XIV. Coalescence of liquid drops in electric and shear fields, J. Colloid Sci. 17 (1962) 383–408.

[20] M. Chabert, K.D. Dorfman, J.L. Viovy, Droplet fusion by alternating current (AC) field electrocoalescence in microchannels, Electrophoresis 26(2005) 3706–3715.

[21] W.D. Ristenpart, J.C. Bird, A. Belmonte, F. Dollar, H.A. Stone, Noncoalescence of oppositely charged drops, Nat. 461 (2009) 377–380.

[22] S.H. Mousavi, M. Ghadiri, M. Buckley, Electro-coalescence of water drops in oils under pulsatile electric fields, Chem. Eng. Sci. 120 (2014) 130–142.

[23] A. Thiam, N. Bremond, J. Bibette, Breaking of an emulsion under an AC electric field, Phys. Rev. Lett. 102 (2009) 188304.

[24] J.C. Bird, W.D. Ristenpart, A. Belmonte, H.A. Stone, Critical angle for electrically driven coalescence of two conical droplets, Phys. Rev. Lett. 103 (2009) 164502.

[25] S.M.Hellesø, P.Atten, G.Berg, L.E.Lundgaard, Experimental study of electrocoalescence of water drops in crude oil using near-infrared camera, Exp. Fluids 56 (2015) 122.

[26] G. Berg, L. Lundgaard, Coalescence efficiency of water drop pairs in oil influenced by electric field, In: 4th international conference on petroleum phase behaviour and fouling, Trondheim, Norway, 2003.

[27] J.A. Melheim, M. Chiesa, S. Ingebrigtsen, G. Berg, Forces between two water droplets in oil under the influence of an electric field, 2004, In: 5th international conference on multiphase Flow, ICMF'4, paper No. 126.

[28] K.W. Warren, New tools for heavy oil dehydration, SPE (2002) 78944.

[29] T. Nishiwaki, K. Adachi, T. Kotaka, Deformation of viscous droplets in an electric field: poly(propylene oxide) poly(dimethy-lsilone) systems, Langmuir 4 (1988) 170-175.

[30] G. I.Taylor, A. D. McEwan, Stability of a horizontal fluid interface in a vertical electric field, J. Fluid Mech. 22 (1965) 1-15.

[31] M.M. Hohman, M. Shin, G. Rutledge, M.P. Brenner, Electrospinning and electrically forced jets, II. Applications. Phys Fluids 13 (2001) 2221–36.

[32] G.H. Xu, W.S. Chen, Breakage of a drop in high-strength electric field, J. Chem. Eng. Chinese Univ. 3 (1994) 221-229.

[33] M. Chiesa, J.A. Melheim, A. Pedersen, S. Ingebrigtsen, G. Berg, Forces acting on water droplets falling in oil under the influence of an electric field: numerical predictions versus experimental observations, Eur. J. Mech. B Fluids 24 (2005) 717–732.

[34] J. Drelich, G. Bryll, J. Kapczynski, J. Hupka, J.D. Miller, F.V. Hanson, The effect of electric field pulsation frequency on breaking water-in-oil emulsions, Fuel Process. Technol. 31 (1992) 105-113.

[35] J.S. Eow, M. Ghadiri, Drop–drop coalescence in an electric field: the effects of applied electric field and electrode geometry, Colloids and Surfaces A: Physicochem. Eng. Aspects 219 (2003) 253–279.

[36] C.L. Herran, N. Coutris, Drop-on-demand for aqueous solutions of sodium alginate, Exp. Fluids 54 (2013) 1-25.